# High-performance radio frequency transistors based on diameter-separated semiconducting carbon nanotubes

Yu Cao, Yuchi Che, Jung-Woo T. Seo, Hui Gui, Mark C. Hersam, and Chongwu Zhou

Citation: Applied Physics Letters **108**, 233105 (2016); doi: 10.1063/1.4953074
View online: http://dx.doi.org/10.1063/1.4953074
View Table of Contents: http://scitation.aip.org/content/aip/journal/apl/108/23?ver=pdfcov
Published by the AIP Publishing



# High-performance radio frequency transistors based on diameter-separated semiconducting carbon nanotubes

Yu Cao,[1,a)] Yuchi Che,[1,a)] Jung-Woo T. Seo,[2,a)] Hui Gui,[3,a)] Mark C. Hersam,[2] and Chongwu Zhou[1,b)]
[1]*Department of Electrical Engineering, University of Southern California, Los Angeles, California 90089, USA*
[2]*Department of Materials Science and Engineering and Department of Chemistry, Northwestern University, Evanston, Illinois 60208, USA*
[3]*Department of Chemical Engineering and Materials Science, University of Southern California, Los Angeles, California 90089, USA*

(Received 1 February 2016; accepted 19 May 2016; published online 8 June 2016)

In this paper, we report the high-performance radio-frequency transistors based on the single-walled semiconducting carbon nanotubes with a refined average diameter of ~1.6 nm. These diameter-separated carbon nanotube transistors show excellent transconductance of 55 $\mu$S/$\mu$m and desirable drain current saturation with an output resistance of ~100 K$\Omega$ $\mu$m. An exceptional radio-frequency performance is also achieved with current gain and power gain cut-off frequencies of 23 GHz and 20 GHz (extrinsic) and 65 GHz and 35 GHz (intrinsic), respectively. These radio-frequency metrics are among the highest reported for the carbon nanotube thin-film transistors. This study provides demonstration of radio frequency transistors based on carbon nanotubes with tailored diameter distributions, which will guide the future application of carbon nanotubes in radio-frequency electronics. *Published by AIP Publishing*. [http://dx.doi.org/10.1063/1.4953074]

Carbon nanotubes, with their unique properties of nanoscale size, high carrier mobility, small intrinsic capacitance, and small intrinsic gate delay,[1–4] are considered to be excellent channel materials for radio frequency (RF) electronics.[1,5–15] The large-scale nanotube films, achieved by dispersing pre-separated high-purity semiconducting nanotube solution, provide the advantages of high semiconducting purity, high density, and scalability, which benefit the nanotube RF electronics. Previously, the RF transistors based on 98% purity semiconducting carbon nanotubes demonstrate extrinsic current gain cut-off frequency ($f_t$) and power gain cut-off frequency ($f_{max}$) of 12 GHz and 8 GHz, respectively.[12] The RF performance of the nanotube transistors based on 99% purity semiconducting carbon nanotubes shows a similar RF performance to the 98% purity semiconducting carbon nanotubes.[16] In order to improve the RF performance of the nanotube thin-film transistors, further engineering of the nanotube parameters is required. Diameter is a critical parameter for carbon nanotubes, as the bandgap of a semiconducting single-walled carbon nanotube (s-SWCNT) is inversely proportional to its diameter.[17] The device parameters of carbon nanotube transistors (e.g., current saturation, carrier mobility, contact resistance, and tube-tube junction resistance) have shown diameter-dependent behavior.[2,3,18–26] As a result, there is a strong motivation to investigate the RF transistors based on the diameter-separated, semiconducting SWCNTs.

In this work, we utilize a self-aligned T-shaped gate structure as the device platform for semiconducting SWCNTs with a refined average diameter of ~1.6 nm. We characterize both the direct current (DC) and RF performance of these transistors. These transistors show excellent transconductance of 55 $\mu$S/$\mu$m, desirable output resistance of ~100 K$\Omega$ $\mu$m, $f_t$ and $f_{max}$ of 23 GHz and 20 GHz (extrinsic) and 65 GHz and 35 GHz (intrinsic), respectively, elucidating the significance of diameter refinement, which provides an effective way to improve the performance of the carbon nanotube RF transistors.

The diameter-refined SWCNTs were isolated using density gradient ultracentrifugation (DGU)[27,28] with a semiconducting purity in excess of 99% and an average diameter of ~1.6 nm,[29] and then used to fabricate the RF transistors with the self-aligned T-shaped gate structures. Fig. 1(a) shows the optical absorbance spectrum of the carbon nanotube solution with a refined average diameter of ~1.6 nm. The narrow peak at ~1100 nm corresponds to carbon nanotubes with ~1.6 nm diameter, which is larger than the average diameters of carbon nanotubes in our previous work (~1.4 nm).[11,12] In the wavelength regime of 600–800 nm, there is only a small peak at ~770 nm that corresponds to the minority species of semiconducting carbon nanotubes with ~1.2 nm diameter, and no other peak corresponding to the metallic nanotubes can be found. The absorbance spectrum thus demonstrates the high degree of diameter and semiconducting refinement of the SWCNTs. The diameter-separated carbon nanotubes were then deposited onto poly-L-lysine-functionalized quartz substrates for device fabrication. In detail, the quartz substrates were first incubated in poly-L-lysine solution for 5 min, washed with de-ionized (DI) water, and blown dry with $N_2$. Then, the diameter-separated carbon nanotube solution was dropped using a pipette onto the quartz substrates, left on the quartz substrates for 10–20 min, rinsed with DI water, and blown dry with $N_2$. Fig. 1(b) shows a scanning electron microscope (SEM) image of a typical carbon nanotube film on a quartz substrate. The nanotube's density is ~10 tubes/$\mu$m$^2$.

[a)]Y. Cao, Y. Che, J.-W. T. Seo, and H. Gui authors contributed equally to this work.
[b)]Author to whom correspondence should be addressed. Electronic mail: chongwuz@usc.edu

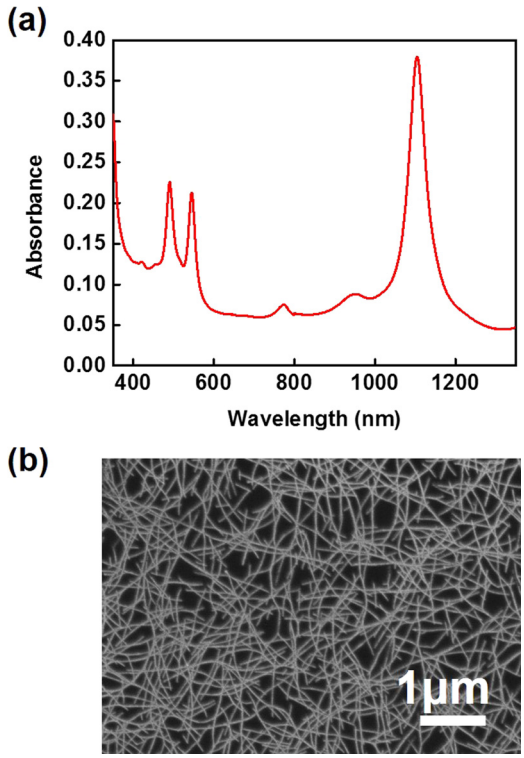


FIG. 1. Characterization of semiconducting single-walled carbon nanotubes with a refined average diameter of ~1.6 nm. (a) Optical absorbance spectrum of the diameter-separated SWCNTs. (b) SEM image of a typical deposited film from the diameter-separated SWCNT solution.

The nanotube film shows a good uniformity and high density, which can enable a large-scale fabrication of the RF transistors, circuits, and systems.[10,11,30]

We then fabricated the self-aligned T-shaped gate RF transistors based on the diameter-separated carbon nanotubes. Fig. 2(a) shows a three-dimensional (3D) schematic of the transistor structure with the T-shaped gate that is designed to reduce the parasitic capacitance, decrease the gate resistance, scale down the channel length, and increase the gate control.[10–12] The fabrication process started with patterning large source and drain electrodes (1 nm titanium and 50 nm gold, shown in yellow in Fig. 2(a)) on the quartz substrates with the diameter-separated carbon nanotubes by photolithography. Second, the active channel regions were defined by photolithography, followed by etching of carbon nanotubes outside the active channel regions. Third, bilayer electron beam resists of different sensitivities (polymethyl methacrylate (PMMA) with 950 k molecular weight as the bottom layer with lower sensitivity, and copolymer of methyl methacrylate and methacrylic acid P(MMA-MAA) as the top layer with higher sensitivity) were used to fabricate the T-shaped gate. The T-shaped gate pattern was formed by exposing a high dose at the gate position center and a low dose at the adjacent area in the same exposure run using an electron beam. After the development of the exposed bilayer resists, 140 nm aluminum was deposited by the thermal evaporator, and the subsequent lift-off process produced the T-shaped gate structure between the source and drain electrodes (shown in red in Fig. 2(a)). The T-shaped gate was then oxidized in air at 120 °C, forming a thin layer of gate dielectric ($Al_2O_3$) with the thickness of 2–4 nm at the interface

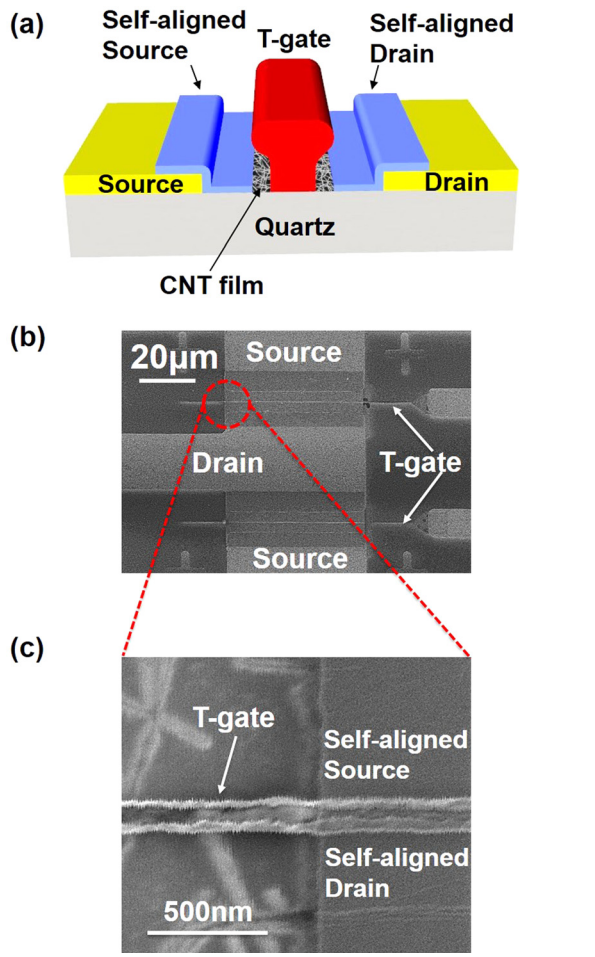


FIG. 2. Device structure of RF transistors based on the carbon nanotubes with a refined average diameter of ~1.6 nm. (a) Schematic of the self-aligned T-shaped gate structure. (b) SEM image of an as-fabricated self-aligned T-shaped gate RF transistor. (c) Close-up SEM image of the T-shaped gate in (b).

between the carbon nanotubes and the aluminum gate electrode due to the diffusion of oxygen to the interface between the carbon nanotubes and the aluminum gate electrode, which has been demonstrated in our previous work.[10–12] In fact, all other exposed area of the aluminum gate would be oxidized to a thin layer of $Al_2O_3$ (2–4 nm). We note that this is different from some previous work which used aluminum as contacts for nanotubes,[18,31] as they did not heat up their devices in air at 120 °C for oxidation. Finally, 10 nm palladium was deposited as the self-aligned source and drain contacts (blue in Fig. 2(a)) to shorten the original separation between the large source and drain electrodes from ~8 $\mu$m to ~160 nm with the T-shaped gate as the hard mask. The channel length ($L$), which is defined by the T-shaped gate foot, is ~120 nm. The un-gated region on each side, which is caused because of the difference in length between the T-shaped gate cap and the T-shaped gate foot, is ~20 nm. Fig. 2(b) shows a top-view SEM image of an as-fabricated self-aligned T-shaped gate transistor, with a close-up image shown in Fig. 2(c).

The DC performance of the as-fabricated, diameter-separated carbon nanotube RF transistors is first characterized. Fig. 3(a) shows the transfer characteristics of a representative transistor with a channel width ($W$) of 50 $\mu$m at a drain-to-source bias ($V_{DS}$) of −1.5 V. The transfer curve exhibits a

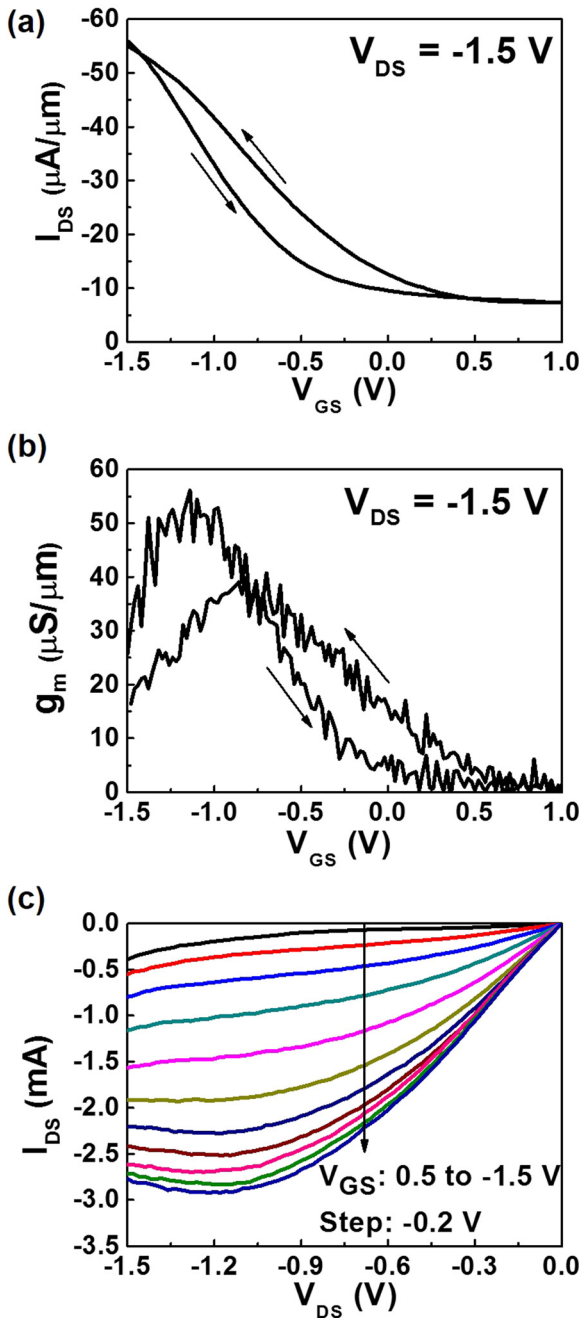


FIG. 3. DC performance of the transistors based on the carbon nanotubes with a refined average diameter of ~1.6 nm. (a) Transfer characteristics ($I_{DS}$–$V_{GS}$ curve) of a representative diameter-separated carbon nanotube transistor at $V_{DS} = -1.5$ V. The channel width ($W$) is 50 $\mu$m. (b) Transconductance ($g_m$–$V_{GS}$ curve) of the same transistor in (a). (c) Output characteristics ($I_{DS}$–$V_{DS}$ curves) of the same carbon nanotube transistor in (a) at various $V_{GS}$ from 0.5 to −1.5 V with a step of −0.2 V.

p-type transistor behavior with hysteresis of ~0.35 V for data points with current value of −15 $\mu$A/$\mu$m, which is common for the carbon nanotube transistors due to charge trapping.[32] The maximum on-current density is ~55 $\mu$A/$\mu$m, which is ~1.5 times larger than previously reported for ultra-high purity semiconducting carbon nanotube transistors (~35 $\mu$A/$\mu$m),[11] and ~2 times larger than 98% purity semiconducting carbon nanotube transistors (~25 $\mu$A/$\mu$m) with the same device structure and similar channel length (~140 nm).[12] We further analyzed the transconductance ($g_m$) of the same transistor by taking the derivative of the transfer curve in Fig. 3(a), with the results being shown in Fig. 3(b). A peak $g_m$ of ~55 $\mu$S/$\mu$m was achieved at a gate-to-source bias ($V_{GS}$) of −1.1 V, which is comparable to the highest value previously reported for the carbon nanotube RF transistors.[10] In comparison, the transconductance was 40 $\mu$S/$\mu$m for ultra-high purity semiconducting carbon nanotube transistors[11] and 20 $\mu$S/$\mu$m for 98% purity semiconducting carbon nanotube transistors with the same device structure and similar channel length (~140 nm).[12] The improved electronic performance in terms of high on-current density and large transconductance is favorable for the RF performance of these diameter-separated carbon nanotube transistors.

The output characteristics of the same transistor are plotted in Fig. 3(c). It can be observed that the drain current of the carbon nanotube transistor begins to saturate when $V_{DS}$ increases beyond −1.1 V. Saturation of the drain current is important for the power gain performance of the RF transistors. The output resistance ($r_o$) of the diameter-separated carbon nanotube transistors can be extracted by using $r_o = \Delta V_{DS}/\Delta I_{DS} \times W$, where $I_{DS}$ is the drain-to-source current. When the change in the drain-to-source current is zero, it yields an infinite output resistance, and the adjacent positive value will be used as the maximum output resistance. The output resistance for the RF transistors based on the diameter-separated carbon nanotubes is extracted to be ~2 kΩ with two data points of $V_{DS} = -1.26$ V and $V_{DS} = -1.24$ V at $V_{GS} = -1.5$ V, which corresponds to ~100 KΩ $\mu$m. For RF electronics, an intrinsic gain above 1 is required to achieve the function of amplification and power gain. For this representative carbon nanotube transistor with a transconductance of 55 $\mu$S/$\mu$m and an output resistance of 100 KΩ $\mu$m, the gain is ~6, confirming that these transistors are qualified for RF amplifier applications. We note that a decrease in current magnitude can be observed when $V_{DS}$ increased negatively from −1.3 V to −1.5 V for the $I_{DS}$-$V_{DS}$ curves with high current magnitude under high negative $V_{GS}$ (from −1.5 V to −0.7 V), while other $I_{DS}$-$V_{DS}$ curves with smaller current and $V_{GS}$ between −0.5 V and 0.5 V did not show such decrease in current magnitude. We suggest that this is due to the self-heating of carbon nanotubes under large current flow.[33] Other factors such as bias stress may deserve further investigation.

We subsequently characterized the RF performance of the self-aligned T-shaped gate transistors based on the carbon nanotubes with a refined average diameter of ~1.6 nm. The ground-signal-ground (GSG) probes with a pitch of 150 $\mu$m and a vector network analyzer (VNA) were utilized for the RF measurements. The entire setup was first calibrated with short-open-load-through (SOLT) standards. We then measured the S-parameter in the frequency range from 50 MHz to 20 GHz. The on-chip open and short structures (see the supplementary material[35]) were also measured for de-embedding purposes. Our de-embedding structures remove the parasitic effects from the bonding pads and the fringe capacitances associated with the gate, and provide the upper-limit of the performance from the carbon nanotubes with a refined average diameter of ~1.6 nm. The current gain ($h_{21}$) and the maximum available power gain ($MAG$) of the carbon nanotube transistors before and after de-embedding were extracted and are shown in Figs. 4(a) and 4(b), respectively. The transistor was biased at $V_{GS} = -1.1$ V and $V_{DS} = -1.5$ V, which were

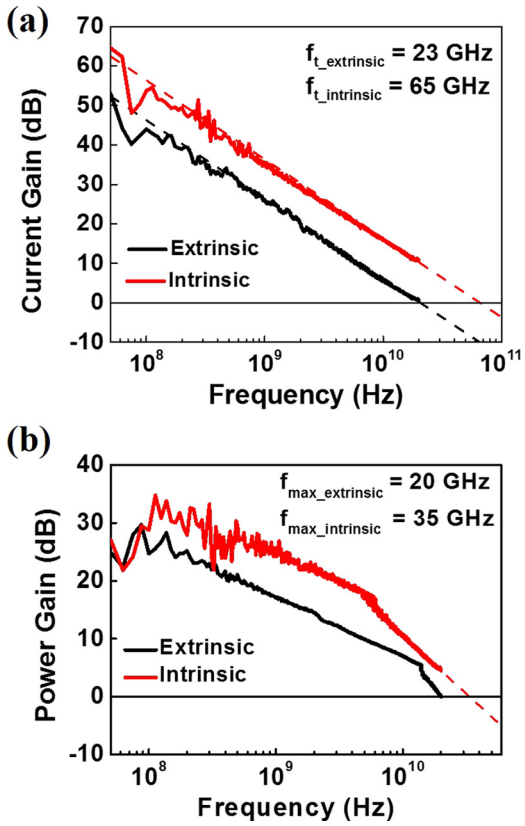


FIG. 4. RF performance of the transistors based on the carbon nanotubes with a refined average diameter of ~1.6 nm. (a) Extrinsic and intrinsic current gain frequency responses. (b) Extrinsic and intrinsic power gain frequency responses.

the conditions with the maximum transconductance and output resistance values. The extrinsic $f_t$ and $f_{max}$ were 23 and 20 GHz, respectively, and the intrinsic $f_t$ and $f_{max}$ were 65 and 35 GHz, respectively. The RF performance, particularly for the $f_{max}$, which is important for practical applications, is comparable to the highest RF performance previously reported for carbon nanotube transistors.[11,13] In previous studies, the best RF transistors based on carbon nanotube thin-films with ultra-high semiconducting purity (99.99%) showed extrinsic $f_t$ and $f_{max}$ of 22 and 19 GHz, respectively,[11] but separation of the 99.99% purity semiconducting carbon nanotubes has an extremely low yield.[34] The best RF transistors based on aligned carbon nanotubes showed extrinsic $f_t$ and $f_{max}$ of 7 and 15 GHz, respectively.[13] The extraordinary RF performance of the transistors based on the diameter-separated carbon nanotubes illustrates the advantages of achieving further diameter separation for carbon nanotube RF electronics, which provides enhancements in both DC and RF device parameters (see the supplementary material for a detailed comparison[35]).

In summary, we have fabricated the self-aligned T-shaped gate RF transistors based on carbon nanotubes with a refined average diameter of ~1.6 nm. These carbon nanotube transistors show excellent maximum transconductance of 55 $\mu$S/$\mu$m and superior drain current saturation with an output resistance of 100 K$\Omega$ $\mu$m. Moreover, the RF measurements exhibit exceptional high frequency performance with $f_t$ of 23 and 65 GHz before and after de-embedding, and $f_{max}$ of 20 and 35 GHz before and after de-embedding. The RF performance of these diameter-separated carbon nanotube RF transistors is among the highest reported for the carbon nanotube transistors, indicating the importance of diameter separation for carbon nanotube radio-frequency electronics. These results are also particularly significant for guiding future studies of high-performance carbon nanotube analog electronics.

We acknowledge the Center for High Frequency Electronics (CHFE) at University of California, Los Angeles for technical support. We thank Mr. Minji Zhu at CHFE for help with RF measurements. We also thank Dr. Han Wang at the University of Southern California for fruitful discussions and Mr. Chenfei Shen at the University of Southern California for help with SEM imaging. J.-W.T.S. and M.C.H. acknowledge support from the National Science Foundation (DMR-1505849) for density gradient ultracentrifugation processing of diameter-refined semiconducting SWCNTs.

[1]C. Rutherglen, D. Jain, and P. Burke, Nat. Nanotechnol. **4**(12), 811 (2009).
[2]T. Dürkop, S. A. Getty, E. Cobas, and M. S. Fuhrer, Nano Lett. **4**(1), 35 (2004).
[3]X. Zhou, J. Y. Park, S. Huang, J. Liu, and P. L. McEuen, Phys. Rev. Lett. **95**(14), 146805 (2005).
[4]A. Javey, J. Guo, Q. Wang, M. Lundstrom, and H. J. Dai, Nature **424**(6949), 654 (2003).
[5]S. D. Li, Z. Yu, S. F. Yen, W. C. Tang, and P. J. Burke, Nano Lett. **4**(4), 753 (2004).
[6]A. Le Louarn, F. Kapche, J. M. Bethoux, H. Happy, G. Dambrine, V. Derycke, P. Chenevier, N. Izard, M. F. Goffman, and J. P. Bourgoin, Appl. Phys. Lett. **90**(23), 233108 (2007).
[7]L. Nougaret, H. Happy, G. Dambrine, V. Derycke, J. P. Bourgoin, A. A. Green, and M. C. Hersam, Appl. Phys. Lett. **94**(24), 243505 (2009).
[8]C. Wang, A. Badmaev, A. Jooyaie, M. Bao, K. L. Wang, K. Galatsis, and C. Zhou, ACS Nano **5**(5), 4169 (2011).
[9]L. Ding, Z. Wang, T. Pei, Z. Zhang, S. Wang, H. Xu, F. Peng, Y. Li, and L. M. Peng, ACS Nano **5**(4), 2512 (2011).
[10]Y. Che, Y. C. Lin, P. Kim, and C. Zhou, ACS Nano **7**(5), 4343 (2013).
[11]Y. Cao, Y. Che, H. Gui, X. Cao, and C. Zhou, Nano Res. **9**(2), 363 (2015).
[12]Y. Che, A. Badmaev, A. Jooyaie, T. Wu, J. Zhang, C. Wang, K. Galatsis, H. A. Enaya, and C. Zhou, ACS Nano **6**(8), 6936 (2012).
[13]M. Steiner, M. Engel, Y. M. Lin, Y. Q. Wu, K. Jenkins, D. B. Farmer, J. J. Humes, N. L. Yoder, J. W. T. Seo, A. A. Green, M. C. Hersam, R. Krupke, and P. Avouris, Appl. Phys. Lett. **101**(5), 053123 (2012).
[14]C. Kocabas, S. Dunham, Q. Cao, K. Cimino, X. Ho, H. S. Kim, D. Dawson, J. Payne, M. Stuenkel, H. Zhang, T. Banks, M. Feng, S. V. Rotkin, and J. A. Rogers, Nano Lett. **9**(5), 1937 (2009).
[15]Z. Wang, S. Liang, Z. Zhang, H. Liu, H. Zhong, L. H. Ye, S. Wang, W. Zhou, J. Liu, Y. Chen, J. Zhang, and L. M. Peng, Adv. Mater. **26**(4), 645 (2014).
[16]Y. Che and C. Zhou, unpublished data.
[17]H. Kataura, Y. Kumazawa, Y. Maniwa, I. Umezu, S. Suzuki, Y. Ohtsuka, and Y. Achiba, Synth. Met. **103**(1–3), 2555 (1999).
[18]Z. Chen, J. Appenzeller, J. Knoch, Y. M. Lin, and P. Avouris, Nano Lett. **5**(7), 1497 (2005).
[19]S. C. Lim, J. H. Jang, D. J. Bae, G. H. Han, S. Lee, I. S. Yeo, and Y. H. Lee, Appl. Phys. Lett. **95**(26), 264103 (2009).
[20]V. Derycke, R. Martel, J. Appenzeller, and P. Avouris, Appl. Phys. Lett. **80**(15), 2773 (2002).
[21]J. Appenzeller, Y. M. Lin, J. Knoch, and P. Avouris, Phys. Rev. Lett. **93**(19), 196805 (2004).
[22]J. L. Zhang, H. Gui, B. L. Liu, J. Liu, and C. W. Zhou, Nano Res. **6**(12), 906 (2013).
[23]Z. Yao, H. W. C. Postma, L. Balents, and C. Dekker, Nature **402**(6759), 273 (1999).
[24]H. W. C. Postma, M. de Jonge, Z. Yao, and C. Dekker, Phys. Rev. B **62**(16), R10653 (2000).
[25]A. N. Andriotis, M. Menon, D. Srivastava, and L. Chernozatonskii, Phys. Rev. Lett. **87**(6), 066802 (2001).
[26]C. Wang, J. Zhang, K. Ryu, A. Badmaev, L. G. De Arco, and C. Zhou, Nano Lett. **9**(12), 4285 (2009).

[27]M. S. Arnold, A. A. Green, J. F. Hulvat, S. I. Stupp, and M. C. Hersam, Nat. Nanotechnol. **1**(1), 60 (2006).
[28]M. C. Hersam, Nat. Nanotechnol. **3**(7), 387 (2008).
[29]J. W. T. Seo, N. L. Yoder, T. A. Shastry, J. J. Humes, J. E. Johns, A. A. Green, and M. C. Hersam, J. Phys. Chem. Lett. **4**(17), 2805 (2013).
[30]H. Chen, Y. Cao, J. Zhang, and C. Zhou, Nat. Commun. **5**, 4097 (2014).
[31]A. Javey, Q. Wang, W. Kim, and H. J. Dai, Tech. Dig. - IEEE Int. Electron Devices Meet. **2003**, 31.2.1–31.2.4.
[32]W. Kim, A. Javey, O. Vermesh, O. Wang, Y. M. Li, and H. J. Dai, Nano Lett. **3**(2), 193 (2003).
[33]E. Pop, D. Mann, J. Cao, Q. Wang, K. E. Goodson, and H. J. Dai, Phys. Rev. Lett. **95**(15), 155505 (2005).
[34]A. Nish, J. Y. Hwang, J. Doig, and R. J. Nicholas, Nat. Nanotechnol. **2**(10), 640 (2007).
[35]See supplementary material at http://dx.doi.org/10.1063/1.4953074 for the open and short structures for the de-embedding process.